

Tuner of heat and electricity ruled by Majorana fermions: the role of the superconducting-metallic boundary phase

L. S. Ricco¹, F. A. Dessotti¹, A. Ramalho², M. S. Figueira³, and A. C. Seridonio^{1,2}

¹*Departamento de Física e Química, Universidade Estadual Paulista, 15385-000, Ilha Solteira, São Paulo, Brazil*

²*Instituto de Geociências e Ciências Exatas - IGCE, Universidade Estadual Paulista, Departamento de Física, 13506-970, Rio Claro, São Paulo, Brazil*

³*Instituto de Física, Universidade Federal Fluminense, 24210-340, Niterói, RJ, Brazil*

We analyze theoretically in a topological U-shaped Kitaev wire, with Majorana fermions (MFs) on the edges, how heat and electricity are sensitive to both the presence of the overlap between these MFs and the asymmetry strength of their couplings $\Delta - t$ and $\Delta + t$ with a single QD, which is embedded with metallic leads. At the low temperature regime, our findings reveal that by changing slightly this asymmetry and increasing the overlap, that the resonance positions of the linear thermal and electrical conductances become entirely tunable as a function of the QD energy level. Furthermore, the thermopower and the figure of merit follow the same trend, as aftermath of the violation in the Wiedemann-Franz law. Such a behavior can be elucidated by evoking an auxiliary fermion: as the pair of the spatially far apart MFs act as a delocalized and regular fermion, this auxiliary fermion emerges as superconducting. Consequently, both the QD and such a fermion are connected not only by the tunneling amplitude t between them, but also exhibit a delocalized Cooper pair split into these states, with binding energy Δ . When Δ deviates slightly from the metallic amplitude t , then the positions of the resonant response in the thermoelectric quantities change drastically. Thereby, the tuner of heat and electricity here proposed is constituted, wherein its operability lies in the vicinity of the superconducting-metallic boundary phase, namely $t = \Delta$. Our results pave the way for an emerging MFs based-mechanism of enhancing/suppressing the heat flux through which we expect to be the still-developed next generation of topological nanodevices.

PACS numbers: 85.35.Be, 74.55.+v, 85.25.Dq

I. INTRODUCTION

Against the proscenium of plenteous phenomena in condensed matter physics, here we catch one fascinating piece of such a set, namely the Majorana fermions (MFs). Manifesting as quasiparticles being equal to their own anti-quasiparticles^{1,2}, they stamp a topological phase of matter that could rise as zero-energy modes, for instance, on the edges of the 1D Kitaev wire³⁻⁷, which is attributed as the most communal toy model for p -wave and spinless topological superconductivity.

Nowadays, MFs are believed to be revealed in semi-conducting nanowires close to s -wave superconducting systems, pierced by perpendicular magnetic fields, respectively from the spin-orbit interaction present in the former and due to an external source. In this way, the spin degree of freedom is quenched and a topological superconducting based-device could be performed⁸. In addition, magnetic chains on top of superconductors with relevant spin-orbit strength^{9,10}, the fractional quantum Hall state with filling factor $\nu = 5/2$ ¹¹, three-dimensional topological insulators¹² and superconducting vortices¹³⁻¹⁵, become entirely promising nests for MFs at the same footing with the toy model for the 1D Kitaev wire.

Noteworthy, once a pair of MFs is spatially separated by distinct boundaries far apart, it reveals the intriguing characteristic that these quasiparticles possess: they can build a nonlocal and robust fermionic *qubit*, emerging decoupled from the host surroundings and free of the

recurring issue of decoherence. Naturally due to that, the hunt for MFs in condensed matter setups has stirred up wide interest from researchers in the fields of quantum information and also in transport context¹⁶⁻¹⁸.

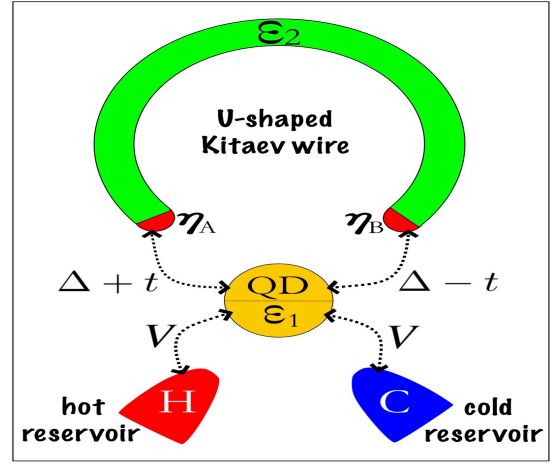


Figure 1. (Color online) Illustration of the device proposed: U-shaped Kitaev wire with MFs η_A and η_B connected by the overlap amplitude ε_2 , which is coupled asymmetrically via $\Delta + t$ and $\Delta - t$ with a QD coupled symmetrically (V) to hot (H) and cold (C) metallic leads. Slight deviations from $t = \Delta$ condition, namely the superconducting-metallic boundary phase, make the setup to behave as tuner of heat and electricity, depending upon the QD energy level.

To the best of our knowledge, these exotic quasiparticles hold the status of innovating candidates for the next generation of technological applications in electronic nanodevices and computing^{19,20}: within the former scenario, some of us have proposed a current switch by employing a couple of quantum dots (QDs)¹⁹, while in the latter we have found bound states in the continuum for the storage of such a *qubit*²⁰. We should mention that in both situations above, a QD is found asymmetrically coupled via $\Delta + t$ and $\Delta - t$ amplitudes to two far apart MFs, in such a way that the aforementioned features are triggered drastically, wondrously just by modifying slightly the asymmetry of couplings.

Particularly, the field of thermoelectricity has experienced a great development in recent years, due to the advances in growth and fabrication of nanoscopic devices. New routes were opened exploring thermoelectric properties of very different systems like quantum dots^{21–24}, nanowires²⁵, superlattices and nanocomposite thermoelectric materials²⁶, ferromagnetic-quantum dot-superconducting device²⁷ and one-dimensional topological Majorana systems^{28,29}.

In this work, by the same manner described previously and based on concrete proposals of thermoelectric detection of MFs^{28,29}, we explore theoretically the zero-bias thermal and electrical transport through a single QD hybridized asymmetrically and symmetrically with MFs and metallic leads, respectively, wherein the MFs lie on the edges of the U-shaped topological Kitaev wire sketched at Fig.1. We have found that, the maximums of the electric and thermal conductances become shifted just by varying slightly the asymmetry of the couplings. Such a possibility of tuning this resonant behavior, in particular, can be perceived solely when these conductances become probed by the energy level of the QD. Farther, we report that the thermopower together with the figure of merit behave similarly, as expected due to the violation in the Wiedemann-Franz law.

Here, to explain our tuner of heat/electricity effect, we benefit from the intriguing property earlier announced concerning the MF nature: as two of them far apart behave, although delocalized, as an unique regular fermion, we demonstrate that the tunability of the resonant behavior here observed can be clarified just by constructing this auxiliary nonlocal fermion, which reflects the natural and collective feature between two overlapped MFs. This turns the system into an equivalent where the pair of MFs become emulated by a superconducting and delocalized fermion state. In this framework, the parameters Δ and t then assume respectively, the role of the Cooper pairing and metallic hopping term amplitudes between the QD and such an auxiliary fermion.

Thereby, the possibility of realizing a simultaneous tuner of heat and electricity rises as feasible, as we demonstrate, operating nearby the superconducting (SC)-metallic boundary phase, namely $\Delta = t$. For future practical and technological applications, we expect that our current results can shed light to an emerging proce-

dures of controlling the heat flux through novel MFs-based topological nanodevices.

II. THE MODEL

To give a theoretical treatment of the setup depicted in Fig.1 describing a U-shaped Kitaev wire within the topological phase and coupled to a QD hybridized to leads, we adopt a Hamiltonian based on the original proposal from Liu and Baranger³⁰:

$$\begin{aligned} \mathcal{H} = & \sum_{\alpha k} \tilde{\varepsilon}_{\alpha k} c_{\alpha k}^\dagger c_{\alpha k} + \varepsilon_1 d_1^\dagger d_1 + V \sum_{\alpha k} (c_{\alpha k}^\dagger d_1 + \text{H.c.}) \\ & + \frac{(t + \Delta)}{\sqrt{2}} (d_1 - d_1^\dagger) \eta_A + i \frac{(\Delta - t)}{\sqrt{2}} (d_1 + d_1^\dagger) \eta_B \quad (1) \\ & + i \varepsilon_2 \eta_A \eta_B, \end{aligned}$$

where the electrons in the lead $\alpha = H, C$ (for hot and cold reservoirs, respectively), are described by the operator $c_{\alpha k}^\dagger$ ($c_{\alpha k}$) for the creation (annihilation) of an electron in a quantum state labeled by the wave number k and energy $\tilde{\varepsilon}_{\alpha k} = \varepsilon_k - \mu_\alpha$, with μ_α as the chemical potential. For the QD coupled to leads, d_1^\dagger (d_1) creates (annihilates) an electron in the state ε_1 . V stands for the hybridizations between the QD and the leads. The QD couples asymmetrically to the U-shaped Kitaev wire with tunneling amplitudes proportional to $t + \Delta$ and $t - \Delta$, respectively for the left and right MFs $\eta_A = \eta_A^\dagger$ and $\eta_B = \eta_B^\dagger$, which are connected to one another via the overlapping amplitude ε_2 . We call attention that amplitudes $1/\sqrt{2}$ and $i/\sqrt{2}$, respectively for $t + \Delta$ and $t - \Delta$, constitute a gauge that turns the second and third lines of Eq. (1) into $t d_1 d_2^\dagger + \Delta d_2^\dagger d_1^\dagger + \text{H.c.} + \varepsilon_2 d_2^\dagger d_2 - \frac{\varepsilon_2^2}{2}$, when the representation $d_2 = \frac{1}{\sqrt{2}}(\eta_A + i \eta_B)$ is used for a nonlocal fermion. As a result, we can notice that the electronic states within d_2 and d_1 beyond the normal tunneling t between them, become bounded as a Cooper pair with binding energy Δ . This mapping, as we will see later on, will be extremely helpful to figure out how a simultaneous tuner of heat and electricity, assisted by MFs, can rise in the setup proposed at Fig. 1.

In what follows, we use the Landauer-Büttiker formula for the zero-bias thermoelectric quantities \mathcal{L}_n ^{28,29}, due to a temperature gradient. Such quantities are given by:

$$\mathcal{L}_n = \frac{1}{h} \Gamma \int d\varepsilon \left(\frac{\partial f_F}{\partial \varepsilon} \right) \varepsilon^n \text{Im}(\tilde{\mathcal{G}}_{d_1 d_1}), \quad (2)$$

where h is the Planck's constant, $\Gamma = 2\pi V^2 \sum_k \delta(\varepsilon - \varepsilon_k)$ is the Anderson broadening³¹, f_F stands for the Fermi-Dirac distribution, $\tilde{\mathcal{G}}_{d_1 d_1}$ is the retarded Green's function for the QD in energy domain ε , obtained from the time Fourier transform of $\tilde{\mathcal{G}}_{AB} = \int d\tau \mathcal{G}_{AB} e^{\frac{i}{h}(\varepsilon + i0^+)\tau}$, where $\mathcal{G}_{AB} = -\frac{i}{h} \theta(\tau) \text{Tr}\{\varrho[\mathcal{A}(\tau), \mathcal{B}^\dagger(0)]_+\}$ corresponds to the Green's function in time domain τ , here expressed in terms of the density matrix ϱ for Eq. (1) dependent upon the temperature T and the Heaviside function $\theta(\tau)$.

Furthermore, we introduced $\mathcal{T} = -\Gamma \text{Im}(\tilde{\mathcal{G}}_{d_1 d_1})$ as the transmittance through the QD, $G = e^2 \mathcal{L}_0$ ($K = (\mathcal{L}_2 - \frac{\mathcal{L}_1^2}{\mathcal{L}_0})/T$) and $S = -\mathcal{L}_1/eT\mathcal{L}_0$, respectively for the electrical (thermal) conductance and thermopower. Here, we explore the violation of the Wiedemann-Franz law given by $WF = K/GT$ in units of the Lorenz number $L_0 = (\pi^3/3)(k_B/e)^2$ and the increasing of the figure of merit $ZT = S^2 GT/K$ as aftermath^{28,29}.

Particularly for Eq.(2), we used the equation-of-motion (EOM) method³² summarized as follows: $(\varepsilon + i0^+)\tilde{\mathcal{G}}_{AB} = [\mathcal{A}, \mathcal{B}^\dagger]_+ + \tilde{\mathcal{G}}_{[\mathcal{A}, \mathcal{H}]\mathcal{B}^\dagger}$ with $\mathcal{A} = \mathcal{B} = d_1$ and calculate $\tilde{\mathcal{G}}_{d_1 d_1}$ together with other Green's functions. As a result, we find

$$(\varepsilon - \varepsilon_1 - \Sigma)\tilde{\mathcal{G}}_{d_1 d_1} = 1 - t\tilde{\mathcal{G}}_{d_2 d_1} - \Delta\tilde{\mathcal{G}}_{d_2^\dagger d_1}, \quad (3)$$

expressed in terms of the self-energy $\Sigma = -i\Gamma$ and Green's functions $\tilde{\mathcal{G}}_{d_2 d_1}$ and $\tilde{\mathcal{G}}_{d_2^\dagger d_1}$. According to the EOM procedure, we determine

$$\tilde{\mathcal{G}}_{d_2 d_1} = + \frac{\Delta\tilde{\mathcal{G}}_{d_1^\dagger d_1}}{(\varepsilon - \varepsilon_2 + i0^+)} - \frac{t\tilde{\mathcal{G}}_{d_1 d_1}}{(\varepsilon - \varepsilon_2 + i0^+)}, \quad (4)$$

$$\tilde{\mathcal{G}}_{d_2^\dagger d_1} = - \frac{\Delta\tilde{\mathcal{G}}_{d_1 d_1}}{(\varepsilon + \varepsilon_2 + i0^+)} + \frac{t\tilde{\mathcal{G}}_{d_1^\dagger d_1}}{(\varepsilon + \varepsilon_2 + i0^+)} \quad (5)$$

and $\tilde{\mathcal{G}}_{d_1^\dagger d_1} = -2t\Delta\tilde{K}\tilde{\mathcal{G}}_{d_1 d_1}$, in which $\tilde{K} = \frac{K_{\text{MFs}}}{\varepsilon + \varepsilon_1 + \Sigma - K_-}$, with $K_{\text{MFs}} = \frac{(\varepsilon + i0^+)}{[\varepsilon^2 - \varepsilon_2^2 + 2i\varepsilon 0^+ - (0^+)^2]}$, $\bar{\Sigma}$ as the complex conjugate of Σ and $K_\pm = \frac{(\varepsilon + i0^+)(t^2 + \Delta^2) \pm \varepsilon_2(t^2 - \Delta^2)}{[\varepsilon^2 - \varepsilon_2^2 + 2i\varepsilon 0^+ - (0^+)^2]}$. Thus substituting Eqs. (4), (5) and those above into Eq.(3), the Green's function of the QD is evaluated as

$$\tilde{\mathcal{G}}_{d_1 d_1} = \frac{1}{\varepsilon - \varepsilon_1 - \Sigma - \Sigma_{\text{MFs}}}, \quad (6)$$

where $\Sigma_{\text{MFs}} = K_+ + (2t\Delta)^2\tilde{K}K_{\text{MFs}}$ accounts for the self-energy arising from the MFs hybridized with the QD.

III. RESULTS AND DISCUSSION

Below we investigate the thermoelectric behavior of the U-shaped topological Kitaev wire depicted at Fig. 1 by assuming $k_B = 1$ (Boltzmann's constant) and energy scaled by the Anderson broadening $\Gamma = 2\pi V^2 \sum_k \delta(\varepsilon - \varepsilon_k)$ ³¹, with $k_B T = 10^{-4}\Gamma$ as the system temperature. The Anderson broadening Γ defines the coupling between the QD and the metallic leads, which is assumed symmetrical for a sake of simplicity.

We begin analyzing the situation wherein solely the MF η_A exists at Fig. 2(a) for several overlapping amplitudes ε_2 , thus characterizing the superconducting-metallic boundary phase $t = \Delta = 4\Gamma$. In such a condition, the terms $d_1 d_2^\dagger + \text{H.c.}$ and $d_2^\dagger d_1^\dagger + \text{H.c.}$ for the auxiliary fermion d_2 compete at the same footing. Fig. 2(a) presents the electrical conductance $G = e^2 \mathcal{L}_0$ in units of the quantum $G_0 = e^2/h$ as a function of the QD energy

level ε_1 . Particularly for isolated MFs due to $\varepsilon_2 = 0$, we verify that G/G_0 attains to the plateau given by 0.5 (half-fermion state) whatever the value of ε_1 (see the black line of this panel). Such a hallmark arises from the leaking effect of the Majorana fermion state into the QD, which appears deeply discussed by one of us in Ref. [33]. It reveals that the MF zero-mode becomes pinned at the Fermi level of the metallic leads. The change of such a behavior is smooth considering weak overlapping $\varepsilon_2 = 0.001\Gamma$ as we verify looking at the green line of the same panel. Then, the case $\varepsilon_2 = 0$ ensures that the electricity through the QD is not sensitive to the probing energy ε_1 and that the nanodevice is not filtering electrical current within a given energy range. Due to the pinning of the MF zero-energy mode at the Fermi energy, this half-fermion state bridges both the hot and cold leads, thus sustaining the electrical current. As a result, the thermal conductance $K/T(G_0 L_0)$ behaves likewise for weak overlapping terms as it appears in Fig. 2(b). Additionally, we have found that by increasing the overlap amplitude ε_2 , a resonance response of heat and electricity is allowed. To that end, the length of the U-shaped Kitaev wire should be reduced.

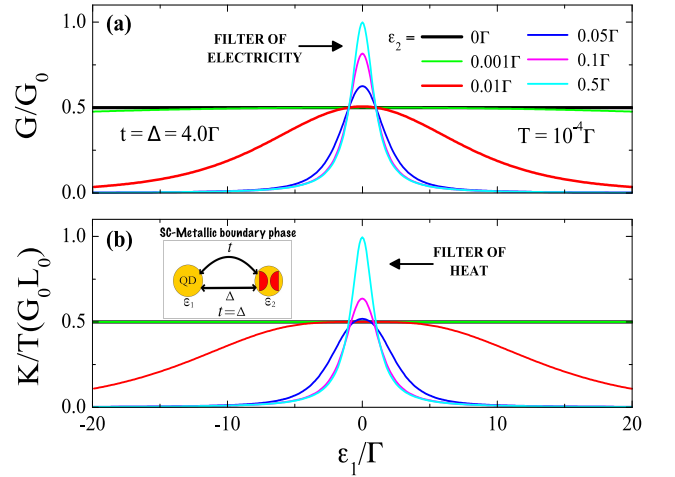


Figure 2. (color online) U-shaped Kitaev wire with just the MF η_A coupled to the QD obtained with $t = \Delta$. (a) Electrical conductance as a function of the QD energy level ε_1 for several overlap amplitudes ε_2 . (b) The same for the thermal conductance. In both cases, heat and electricity are filtered nearby the Fermi energy $\varepsilon_1 = 0$, when the far apart MFs considered are connected ($\varepsilon_2 \neq 0$). Otherwise, such conductances exhibit flat behaviors. In the inset, we visualize the auxiliary fermion made by the MFs η_A and η_B , which appear depicted as half-spheres in red.

By performing that, the resonant response of both thermal $K/T(G_0 L_0)$ and electrical G/G_0 conductances exhibit an exceeding amplitude over the plateau 0.5 of an isolated MF, in particular, in the vicinity of the Fermi level $\varepsilon_1 = 0$. To understand such a characteristic, we should use the interpretation provided by the auxiliary fermion d_2 , in which the overlap amplitude ε_2 plays the

role of its energy level described by the term $\varepsilon_2 d_2^\dagger d_2$. To notice that, see also the inset of Fig. 2(b), wherein the half-spheres depicted in red denote the MFs η_A and η_B as the building blocks of the auxiliary fermion.

Thus, the increasing of ε_2 moves it away from the Fermi energy of the leads and the conductances $K/T(G_0 L_0)$ and G/G_0 evolve to maximum values just for the probing energy ε_1 at resonance with the Fermi energy. Otherwise, such conductances decay and become suppressed. In this way, filters of heat and electricity emerge. At the point $\varepsilon_1 = 0$, the nanodevice is transparent for heat and electricity, respectively with $K/T(G_0 L_0) = 1$ and $G/G_0 = 1$ for highly hybridized MFs, as for instance the case $\varepsilon_2 = 0.5\Gamma$.

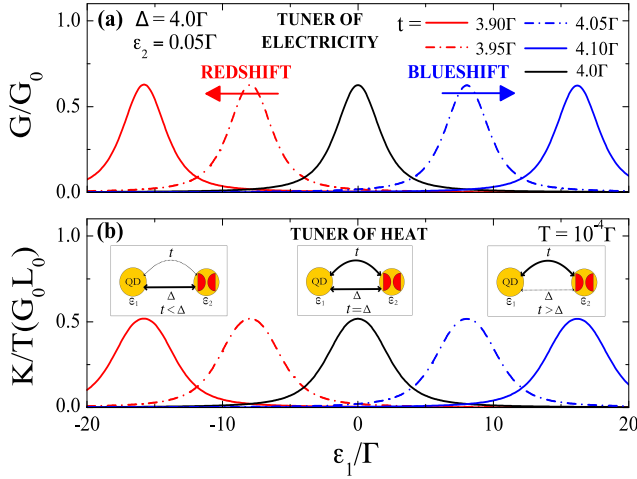


Figure 3. (color online) For slight deviations from the superconducting-metallic boundary phase $t = \Delta$, we find a tuner of: (a) electricity and (b) heat. In (a), the resonant response of the electrical conductance exhibits blueshift for $t > \Delta$ and redshift for $t < \Delta$ as a function of the QD energy level ε_1 . Panel (b) shows the same behavior for the thermal conductance, with insets making explicit the collective behavior of the overlapped MFs η_A and η_B (half-spheres in red).

Once filters of thermoelectric conductances depend upon the QD energy level become allowed, the way that we have found to tune the resonant response is to deviate from the superconducting-metallic boundary phase $t = \Delta = 4\Gamma$. Thus by slight changes in t by keeping constant Δ , which represent the increasing in the asymmetry of couplings $t + \Delta$ and $t - \Delta$ of the MFs with the QD in Fig. 1, the aforementioned filters are finally turned into tuners of electricity and heat, as seen respectively at Figs. 3(a) and (b). Notice that, in these latter panels, blueshift (displacement towards above the leads Fermi level) of the resonant response in the thermoelectric conductances $K/T(G_0 L_0)$ and G/G_0 appear when $t > \Delta$, while redshift in the opposite domain. We make clear that the underlying physical mechanism of such a phenomenon is within the self-energy K_+ , where we can clearly perceive that just when $\varepsilon_2 \neq 0$ together with $t \neq \Delta$, the term $\varepsilon_2(t^2 - \Delta^2)$ in K_+ is relevant and

the rigid shifts of the conductances become allowed.

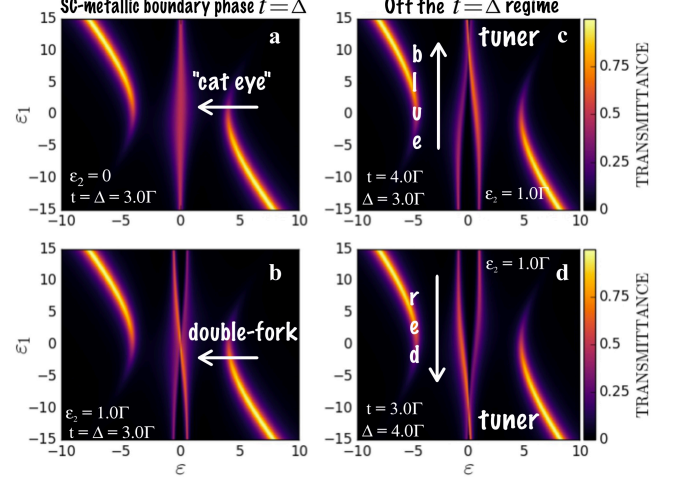


Figure 4. (color online) Transmittance spanned by the axes of ε_1 and ε . Panels (a) and (b) show the regime $t = \Delta$, respectively for $\varepsilon_2 = 0$, which is characterized by a “cat eye”-shaped structure nearby the Fermi level and finite ε_2 , with a double-fork profile instead. In panels (c) and (d), blueshift and redshift are observed when considering $t \neq \Delta$. In this way, the device is turned into a simultaneous tuner of heat and electricity, being the shift of the double-fork profile its hallmark. The arcs are poles from the Green’s function of the QD.

Here, our main remark is that Fig. 3(b) contains the most representative finding of this work: looking at the insets of Fig. 3, the blueshift is observed when the electrons split into the orbitals d_1 and d_2 , prefer to conduct via the hopping t (continuous line in the most right inset) than to stay bounded as a delocalized Cooper pair with binding energy Δ (bold dashed line). In this situation, the device favors the filtering of heat and electricity through the QD at higher energies. In contrast, the redshift holds for the case of Δ (continuous line in the most left inset) overcoming the conduction t (bold dashed line), wherein the filtering phenomenon is reversed towards lower energies, once the electrons split into the above orbitals prefer to stay locked into them. Therefore, our analysis reveals that, it is enough just a minor imbalance between the channels t and Δ to define in which energy domain the system tunes itself for conduction. In what follows, we summarize the tuner of heat/electricity phenomenon here addressed by showing density plots concerning the transmittance $\mathcal{T} = -\Gamma \text{Im}(\tilde{G}_{d_1 d_1})$ spanned by the axes of ε_1 and ε .

Fig. 4 exhibits in panels (a) and (b) the regime $t = \Delta$. In the former panel, we can recognize a central structure in “cat eye”-shaped at $\varepsilon = 0$ and spread along the axis for ε_1 by considering $\varepsilon_2 = 0$ with \mathcal{T} does not exceeding half (0.5), as a result of the half-fermion state due to the MF η_A . However, by taking into account ε_2 finite as in panel (b), the central structure of (a) turns into a double-fork profile, wherein the upper and lower parts of the original

“cat eye”-shaped split, being solely the point $\varepsilon = \varepsilon_1 = 0$ preserved, but with \mathcal{T} overcoming half just in order to filter electrons at the Fermi energy. Off the regime $t = \Delta$ as in panels (c) and (d) of the same figure, the double-fork profile is shifted depending upon if $t > \Delta$ (panel (c) with blueshift pointed out by the up arrow) or $t < \Delta$ (panel (d) with redshift denoted by the down arrow). It is worth mentioning that, in all panels (a)-(d), we can visualize arcs aside the Fermi energy $\varepsilon = 0$, which indeed represent the poles from the Green’s function of the QD.

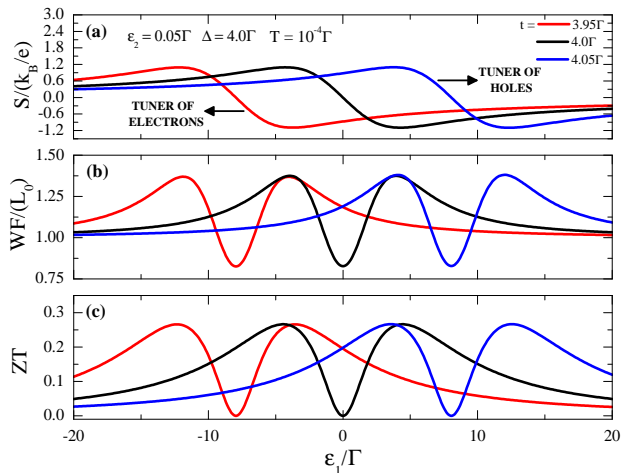


Figure 5. (color online) Other thermoelectric properties as (a) the thermopower (S), (b) the Wiedemann-Franz law (WF) and (c) the figure of merit (ZT) are tuned by deviating slightly from the phase $t = \Delta$. In (a), a highly efficient filter of holes or electrons emerges.

As a consequence, the resonant response of other thermoelectric quantities as the thermopower (S), the Wiedemann-Franz law (WF) and the figure of merit (ZT) found in Fig.5, can also be tuned by deviating slightly from the boundary phase $t = \Delta$. Thus depending upon the regime, if $t > \Delta$ the setup behaves as a tuner of holes due to $S > 0$ or electrons for $S < 0$. Besides, as we can see in Fig.5(b), the violation of the WF law leads

to the enhancement of the ZT (Fig.5(c)). We highlight that, according to the value of the thermopower S , in the domain of the blueshift for Fig.5(a), the majority contribution to the heat flux arises from holes, as we can see in the case $t = 4.05\Gamma$ if considering that the area under the curve is predominantly positive. For $t = 3.95\Gamma$ within the redshift domain, a negative area is dominant, thus pointing out that electrons mostly are the carriers for the thermal current. Remarkably, we realize that in both situations, the minority carrier population of the heat flux can be almost extinguished, just by tuning the system deeply into the blueshift or redshift energy ranges, where respectively, a highly efficient filter of holes or electrons is observed.

IV. CONCLUSIONS

In summary, we have explored theoretically in the zero-bias regime, the proposal of a tuner of heat and electricity in a MFs based-device as depicted at Fig.1. We discuss that such a tuning is feasible by fixing the coefficients Δ and varying t with the single QD coupled to leads, which corresponds to deviate from the superconducting-metallic boundary phase $\Delta = t$ of the auxiliary fermion composed by the MFs. This feature can be achieved considering a finite overlap between the MFs and by evaluating the thermoelectric quantities as a function of the QD energy level. In addition, the thermopower, Wiedemann-Franz law as well as the figure of merit behave similarly as we have checked. Therefore, our findings point out that besides the allowed control of the electronic current assisted by topological MFs, they also reveal a novel mechanism for enhancing/suppressing the heat flux through nanodevices.

ACKNOWLEDGMENTS

This work was supported by the Brazilian agencies CNPq, CAPES and 2015/23539-8 São Paulo Research Foundation (FAPESP).

- ¹ J. Alicea, Rep. Prog. Phys. **75**, 076501 (2012).
- ² S. R. Elliott and M. Franz, Rev. Mod. Phys. **87**, 137 (2015).
- ³ A. Y. Kitaev, Phys. Usp. **44**, 131 (2001).
- ⁴ A. A. Zyuzin, D. Rainis, J. Klinovaja, and D. Loss, Phys. Rev. Lett. **111**, 056802 (2013).
- ⁵ D. Rainis, J. Klinovaja, L. Trifunovic, and D. Loss, Phys. Rev. B **87**, 024515 (2013).
- ⁶ A. Zazunov, P. Sodano, and R. Egger, New J. Phys **15**, 035033 (2013).
- ⁷ D. Roy, C. J. Bolech, and N. Shah, Phys. Rev. B **86**, 094503 (2012).
- ⁸ V. Mourik, K. Zuo, S. M. Frolov, S. R. Plissard, E. P. A. M. Bakkers, and L. P. Kouwenhoven, Science **336**, 1003

- (2012).
- ⁹ S. N.- Perge, I. K. Drozdov, J. Li, H. Chen, S. Jeon, J. Seo, A. H. MacDonald, B. A. Bernevig, and A. Yazdani, Science **346**, 602 (2014).
- ¹⁰ R. Pawlak, M. Kisiel, J. Klinovaja, T. Meier, S. Kawai, T. Glatzel, D. Loss, and E. Meyer, arXiv:1505.06078v2 (2015).
- ¹¹ G. Moore, and N. Read, Nucl. Phys. **B360**, 362 (1991).
- ¹² L. Fu, C. L. Kane, and E. J. Mele, Phys. Rev. Lett. **98**, 106803 (2007).
- ¹³ L. Fu and C.L. Kane, Phys. Rev. Lett. **100**, 096407 (2008).
- ¹⁴ J. D. Sau, R. M. Lutchyn, S. Tewari, and S. Das Sarma, Phys. Rev. Lett. **104**, 040502 (2010).

- ¹⁵ T. Kawakami and X. Hu, Phys. Rev. Lett. **115**, 177001 (2015).
- ¹⁶ K. Flensberg, Phys. Rev. Lett. **106**, 090503 (2011).
- ¹⁷ M. Leijnse and K. Flensberg, Phys. Rev. Lett. **107**, 210502 (2011).
- ¹⁸ M. Leijnse and K. Flensberg, Phys. Rev. B **86**, 134528 (2012).
- ¹⁹ F. A. Dessotti, L. S. Ricco, Y. Marques, L. H. Guessi, M. Yoshida, M. S. Figueira, M. de Souza, Pasquale Sodano, and A. C. Seridonio, Phys. Rev. B **94**, 125426 (2016).
- ²⁰ L. S. Ricco, Y. Marques, F. A. Dessotti, R. S. Machado, M. de Souza, and A. C. Seridonio, Phys. Rev. B **93**, 165116 (2016).
- ²¹ R. Scheibner, H. Buhmann, D. Reuter, M. N. Kiselev, L. W. Molenkamp, Phys. Rev. Lett. **95**, 176602 (2005).
- ²² R. Scheibner, E. G. Novik, T. Borzenko, M. König, D. Reuter, A. D. Wieck, H. Buhmann, L. W. Molenkamp, Phys. Rev. B **75**, 041301 (2007).
- ²³ S. F. Svensson, A. I. Persson, E. A. Hoffmann, N. Nakpathomkun, H. Q. Xu, H. A. Nilsson, H. Q. Xu, L. Samuelson, and H Linke, New Journal of Physics, **14**, 033041 (2012).
- ²⁴ S. Donsa, S. Andergassen, and K. Held, Phys. Rev. B **89**, 125103 (2014).
- ²⁵ E. A. Hoffmann, H. A. Nilsson, J. E. Matthews, N. Nakpathomkun, A. I. Persson, L. Samuelson, and H. Linke, Nano Letters **9**, 779 (2009).
- ²⁶ M. S. Dresselhaus, G. Chen, M. Y. Tang, R. Yang, H. Lee, D. Wang, Z. Ren, J.-P. Fleurial, and P. Gogna, Adv. Materials **19**, 1043 (2007).
- ²⁷ S.-Y. Hwang, R. López, and D. Sánchez, Phys. Rev. B **94**, 054506 (2016).
- ²⁸ J. P. R. -Andrade, O. Á.- Ovando, P. A. Orellana, S. E. Ulloa, Phys. Rev. B **94**, 155436 (2016).
- ²⁹ R. López, M. Lee, L. Serra, and J. S. Lim, Phys. Rev. B **89**, 205418 (2014).
- ³⁰ D. E. Liu and H. U. Baranger, Phys. Rev. B **84**, 201308(R) (2011).
- ³¹ P. W. Anderson, Phys. Rev. **124**, 41 (1961).
- ³² H. Haug and A. P. Jauho, Quantum Kinetics in Transport and Optics of Semiconductors, Springer Series in Solid-State Sciences 123 (Springer, New York, 1996).
- ³³ E. Vernek, P. H. Penteado, A. C. Seridonio, and J.C. Egues, Phys. Rev. B **89**, 165314 (2014).